A Novel Synthesis of Sol−Gel Hybrid Materials by a Nonhydrolytic/Hydrolytic Reaction of (3-Glycidoxypropyl)trimethoxysilane with $TiCl_4$

P. Innocenzi,*[,†] A. Sassi,[‡] G. Brusatin,[†] M. Guglielmi,[†] D. Favretto,[§] R. Bertani,[§] A. Venzo,[§] and F. Babonneau[||]

Dipartimento di Ingegneria Meccanica, Settore Materiali, Università di Padova, via Marzolo 9, 35131 Padova, Italy, Dipartimento di Processi Chimici dell'Ingegneria, Università di Padova, via Marzolo 9, 35131 Padova, Italy, Centro di Chimica Metallorganica del CNR, Istituto di Chimica Industriale, Università di Padova, via Marzolo 9, 35131 Padova, Italy, and Chimie de la Matière Condensée, Université Paris 6, T54-E5, 4 place Jussieu, 75252 Paris Cedex 05, France

Received February 6, 2001. Revised Manuscript Received April 10, 2001

(3-Glycidoxypropyl)trimethoxysilane (GPTMS) derived hybrid organic−inorganic materials have been obtained by a new multistep nonhydrolytic/hydrolytic synthesis. The new synthesis has been achieved using titanium(IV) chloride instead of titanium alkoxides to catalyze the epoxy ring opening in the organically modified alkoxide. The precursor sols were studied by multinuclear solution-state magnetic resonance (NMR) techniques, gas chromatography coupled with mass spectrometry (GC-MS), and electrospray ionization (ESI) experiments. The derived powdered gels were characterized by multinuclear solid-state magic angle spinning (MAS) NMR, Fourier transform infrared (FT-IR), and matrix-assisted laser desorption/ionization (MALDI) experiments. All these results show that epoxy ring opening is achieved at low temperature and within short reaction times. Interestingly, several reactions occur simultaneously and are involved in the early polymerization process, leading to fast catalyst deactivation in solution, chlorination of GPTMS organic groups, and titanium dispersion inside precursor sols. Despite a rather complex reaction pathway, this method can be used to prepare transparent hybrid organic−inorganic materials, whose properties can satisfy the requirements for photonic applications.

Introduction

(3-Glycidoxypropyl)trimethoxysilane (GPTMS) is one of the most common precursors for the preparation of hybrid organic−inorganic materials.[1−3] Several important applications have been reported for these materials in many different fields, for instance as protective layers on organic polymers, membranes,[4] solid electrolytes,[5] and antifogging and anticorrosion coatings. Another very important application is in photonics. GPTMS has been used to fabricate hybrid materials for optical waveguides,[6,7] optical limiting,[8] and optical amplification.[9]

A basic requirement of the materials to be used in photonics is a very high homogeneity at the molecular level. This property is fundamental when the hybrid materials are used as host matrixes for optically active functional molecules, as in the case of fullerenes[8] or push−pull chromophores.[10] Aggregation of the guest molecules should, in fact, be avoided to preserve their optical properties, and this can only be achieved if the microstructure of the matrix is homogeneous enough to ensure a very high dispersion of the doping molecules. A high homogeneity is also necessary when the device has an optoelectronic configuration to minimize optical losses of propagation.

GPTMS is an organically modified alkoxide containing an epoxide ring. The opening of epoxy rings allows

† Dipartimento di Ingegneria Meccanica, Settore Materiali, Università di Padova.

‡ Dipartimento di Processi Chimici dell'Ingegneria, Università di Padova.

§ Centro di Chimica Metallorganica del CNR, Istituto di Chimica Industriale, Università di Padova.

|| Chimie de la Matière Condensée, Université Paris 6.

(1) Schmidt, H. *Mater. Res. Soc. Symp.* **1984**, *32*, 327.
(2) Schmidt, H. *J. Non-Cryst. Solids* **1994**, *178*, 302.
(3) Schmidt, H. *J. Sol-Gel Sci. Technol.* **1997**, *8*, 557.
(4) Sforca, M. L.; Yoshida, I. V. P.; Nunes, S. P. *J. Membr. Sci.* **1999**, *159*, 197.
(5) Popall, M.; Durand, H. *Electrochim. Acta* **1992**, *37*, 1593.
(6) Sorek, Y.; Zevin, M.; Reisfeld, R.; Hurvits, T.; Rushin, S. *Chem. Mater.* **1997**, *9*, 670.
(7) Innocenzi, P.; Martucci, A.; Guglielmi, M.; Armelao, L.; Battaglin, G.; Pelli, S.; Righini, G. C. *J. Non-Cryst. Solid* **1999**, *259*, 189.
(8) (a) Signorini, R.; Meneghetti, M.; Bozio, R.; Maggini, M.; Scorrano, G.; Prato, M.; Brusatin, G.; Innocenzi, P.; Guglielmi, M. *Carbon* **2000**, *38*, 1653. (b) Innocenzi, P.; Brusatin, G.; Guglielmi, M.; Signorini, R.; Meneghetti, M.; Bozio, R.; Maggini, M.; Scorrano, G.; Prato, M. *J. Sol-Gel Sci. Technol.* **2000**, *19*, 263. (c) Innocenzi, P.; Brusatin, G.; Guglielmi, M.; Signorini, R.; Bozio, R.; Maggini, M. *J. Non-Cryst. Solids* **2000**, *265*, 68. (d) Brusatin, G.; Innocenzi, P.; Guglielmi, M.; Bozio, R.; Meneghetti, M.; Signorini, R.; Maggini, M.; Scorrano, G.; Prato, M. *SPIE* **1999**, *3803*, 90.
(9) Casalboni, A.; De Matteis, F.; Prosposito, P.; Pizzoferrato, R. *Appl. Phys. Lett.* **1999**, *75*, 2172.
(10) Abbotto, A.; Bozio, R.; Brusatin, G.; Facchetti, A.; Guglielmi, M.; Innocenzi, P.; Meneghetti, M.; Pagani, G. A.; Signorini, R. *SPIE* **1999**, *3803*, 18.

10.1021/cm011034o CCC: $20.00
Published on Web 09/15/2001

the formation, under particular conditions, of a poly(ethylene oxide) chain. Several syntheses have been reported for these alkoxides, under either acidic[2,11] or basic conditions.[12,13] As previously stated, GPTMS-based hybrids are among the most successful organic−inorganic materials, and the first papers on this subject were published at the beginning of the 1980s.[1,11,14] More recently, however, the synthesis and microstructure of this family of materials have been critically reconsidered with a better understanding of their fundamental properties. In particular, it has become clear that some critical points in the synthesis have been previously overlooked.[15−17] The first is that the simultaneous polymerization of the inorganic and organic network is a competitive process; a faster polycondensation rate of the inorganic network hinders the polymerization of the organic network and vice versa.[16] This process can be controlled by the amount and nature of reaction promoter or catalyst employed.

A second important issue is the role played in the synthesis by water and alcoholic solvent.[15] The alcohol is the solvent used to dissolve GPTMS, and water is used for the hydrolysis and polycondensation process of the inorganic side. The presence of water and alcohols in the synthesis has the final effect to reduce the formation of poly(ethylene oxide) units and to lower the degree of control in the final microstructure.[17,18] The epoxides, in fact, can react with water in acidic conditions or, for instance, with methanol to form diols or methyl ether terminal groups.[15]

It is important to note that the most common synthetic routes to prepare GPTMS-based materials employed transition metal alkoxides, such as titanium,[14,17] aluminum[15] or zirconium[6,14] alkoxides. These alkoxides play a double role: catalysts for epoxy ring opening and inorganic network formers. At the same time titanium or zirconium alkoxides contribute to design the material properties, such as refractive index and scratch resistance. The high reactivity of these metal alkoxides, however, needs to be carefully controlled, for example, by addition of chelating ligands in the precursor sol. Unfortunately, these organic molecules are not easily removed from the final material and can reduce the optical quality required for photonic applications. This is particularly critical when titanium alkoxides are used in the synthesis. In this case, even if chelating ligands are added and a careful control of the synthesis is used, the formation of titania clusters, which produces a phase separation within the matrix, cannot be avoided. The presence of these clusters reduces the microstructural homogeneity thus increasing the optical loss and also limiting the possibility to reach a very homogeneous dispersion of organic doping molecules in the matrix. In previous works we have introduced fullerene derivatives in GPTMS matrixes synthesized with $TiCl_4$, instead of titanium alkoxides. This synthesis has been performed by a multistep process, adding $TiCl_4$ to GPTMS in nonhydrolytic conditions to achieve the organic polymerization. Water and alcohol have been mixed in a second step to form the inorganic network. Much improved optical limiting performances have been obtained with respect to GPTMS materials prepared with titanium alkoxides. We have attributed these improved properties to a larger microstructural homogeneity of the host matrix that prevents aggregation of fullerenes and increases the laser damage resistance of the system.

In the present work we have specifically studied the synthesis of GPTMS-based materials via nonhydrolytic/hydrolytic reactions of (3-glycidoxypropyl)trimethoxysilane with $TiCl_4$. This synthesis has been developed with the aim of overcoming some of the difficulties experienced in the synthesis of this family of hybrid materials, to enhance the optical performances of GPTMS based materials in photonics applications, and to increase the overall knowledge of the microstructure of these solids. This paper is the third of a series of specific studies on this subject.[16,19]

Experimental Section

Materials. (3-Glycidoxypropyl)trimethoxysilane and titanium(IV) chloride were analytical grade and purchased from Aldrich. Dichloromethane was dried by distillation over calcium hydride. 2-Propanol (Aldrich) was used as the solvent and bidistilled water for hydrolysis.

Synthesis of the Precursor Sol. The synthesis was achieved in three steps. In the first step $TiCl_4$ was added under reflux to GPTMS in CH_2Cl_2 (GPTMS:CH_2Cl_2 = 1:5). This solution was stirred for 1 h at 60 °C (step 1: epoxide ring opening). Two different molar ratios of the reagents were used: GPTMS:$TiCl_4$ = 8:1 (sol **GTi1**) or GPTMS:$TiCl_4$ = 4:1 (sol **GTi2**). The reaction was followed by NMR in various experimental conditions, adding $TiCl_4$ at room temperature or at −10 °C. The low-temperature reactions were performed in a hermetically closed flask.

For the second step the sol was diluted, at room temperature, by excess Pr^iOH with respect to $TiCl_4$ (molar ratio Pr^iOH:$TiCl_4$ = 11:1) and stirred for 2 h at 60 °C (step 2: precondensation). All the preparations in steps 1 and 2 were carried out under N_2, using oven-dried vessels.

In the final step water was added dropwise at room temperature to the solution (molar ratio H_2O:GPTMS = 1:1). The mixture was then stirred at room temperature for 3 h (step 3: hydrolysis−condensation).

Monolithic gel **GTi1** was obtained by putting the solution in a PET container maintained at 40 °C for 2 days and at 60 °C for 1 day. The final bulk material was finely ground to obtain powder for the MAS NMR and FTIR and dried again at 60 °C before analysis.

Coating films were deposited from fresh **GTi1** sols (after the final step 3 of preparation) by dip-coating on silica glass substrates. The samples were thermally treated in air at 120 °C for 1 h.

To prepare reference powder samples, another sol (GT) was also prepared as described in ref 19. This was achieved simply by refluxing GPTMS with tetraethyl orthosilicate (TEOS) in acidic conditions with the following molar ratios: GPTMS:TEOS = 7:3; (GPTMS + TEOS):H_2O:HCl:MeOH = 1:3.3:0.004:0.013. Powders were prepared by drying a bulk gel in a thermostatic chamber for 1 day at 60 °C.

(11) Schmidt, H. *J. Non-Cryst. Solids* **1985**, *73*, 681.
(12) Popall, M.; Durand, H. *Electrochim. Acta* **1992**, *37*, 1593.
(13) Riegel, B.; Blittersdorf, S.; Kiefer, W.; Hofacker, S.; Muller, M.; Schottner, G. *J. Non-Cryst. Solids* **1998**, *226*, 76.
(14) Philipp, G.; Schmidt, H. J. *Non-Cryst. Solids* **1986**, *82*, 31.
(15) Templin, M.; Wiesner, U.; Spiess, H. W. *Adv. Mater.* **1997**, *9*, 814.
(16) Innocenzi, P.; Brusatin, G.; Babonneau, F. *Chem. Mater.* **2000**, *12*, 3726.
(17) Hoebbel, D.; Nacken, M.; Schmidt, H. *J. Sol-Gel Sci. Technol.* **1998**, *12*, 169.
(18) Hoebbel, D.; Nacken, M.; Schmidt, H. *J. Sol-Gel Sci. Technol.* **1998**, *13*, 37.
(19) Innocenzi, P.; Brusatin, G.; Guglielmi, M.; Bertani, R. *Chem. Mater.* **1999**, *11*, 1672.

Solution NMR. Multinuclear NMR characterization were performed on a Bruker AC200 spectrometer operating at 200.13 MHz for ^{1}H, 50.32 MHz for ^{13}C, and 39.76 MHz for ^{29}Si. All NMR measurements were performed using CD_2Cl_2, which was used as received, in 1:1 solvent/reaction mixture samples. ^{1}H and ^{13}C chemical shifts were calibrated against CD_2Cl_2 residual resonance multiplet (for ^{1}H 5.31 ppm; for ^{13}C 53.73 ppm) and were referenced to tetramethylsilane (TMS) at 0 ppm. Both {^{1}H} broad-band decoupled and coupled ^{13}C NMR spectra were recorded. ^{29}Si chemical shifts were calibrated using an external standard of tetramethylsilane at 0 ppm. Reported ^{29}Si NMR spectra were collected with a recycle delay of 180 s, avoiding the use of relaxing agents added to the reaction mixture.

Two-Dimensional NMR. The ^{1}H and ^{13}C NMR spectra were obtained on a Bruker Avance-400 spectrometer operating at 400.13 and 100.61 MHz, respectively. The assignments of the proton resonances were performed by standard chemical shift correlations and homonuclear COSY and NOESY experiments. The ^{13}C resonances were attributed through 2D-heterocorrelated COSY experiments (HMQC with bird sequence[20] and quadrature detection along F1 achieved using the TPPI method[21]).

Solid-State NMR. The ^{29}Si MAS NMR and ^{13}C CP MAS NMR spectra were recorded with a MSL300 Bruker spectrometer at 59.63 and 75.47 MHz, respectively, using a CP-MAS Bruker probe equipped with 7 mm ZrO_2 rotors, spinning at 4 kHz. The following acquisition parameters were used for ^{29}Si: spectral width of 20 kHz; 2K data points; pulse width of 2 μs ($\theta \approx 30°$); recycle delay of 60 s. A 50 Hz exponential broadening was applied before Fourier transform. The ^{13}C CP MAS NMR spectra were recorded under the same Hartmann−Hahn match condition, set up by using a powdered sample of adamantane: both rf channel levels $\omega^1_H/2\pi$ and $\omega^{13}_C/2\pi$ were adjusted so that $|\omega^1_H|/2\pi = |\omega^{13}_C|/2\pi = 43$ kHz. Proton decoupling was applied during acquisition. A contact time of 3 ms was used, with a spectral width of 20 kHz and 1K data points. A 20 Hz exponential broadening was applied before Fourier transform. ^{29}Si and ^{13}C NMR spectra were referenced externally to TMS at 0 ppm.

GC/MS Analysis. GC/MS determinations were performed on a QMD 1000 instrument: column PS264, 30 mL; He flow 1 mL min^{-1}; temperature from 100 to 280 °C, 10 °C min^{-1}.

ESI Analysis. Electrospray ionization (ESI) experiments were performed on a LCQ (Thermoquest, San José, CA) ion trap instrument equipped with an electrospray ion source. The instrument was operated in the positive ion mode, with spray voltage of 4.3 kV, capillary temperature 150 °C, N_2 sheath gas flow 40 (au). Samples were dissolved in CH_2Cl_2 and supplied to the ESI source by syringe infusion at 5 μL min^{-1}.

MALDI Analysis. Matrix-assisted laser desorption/ionization (MALDI) measurements were performed on a Reflex time-of-flight instrument (Bruker-Franzen Analytik, Bremen, Germany), operating in the positive-ion linear mode. Ions formed by a pulsed UV laser beam (nitrogen laser, $\lambda = 337$ nm) were accelerated to 25 keV. A fine powder was obtained from solid samples, suspended in $CHCl_3$. A 5 μL volume of this suspension was mixed with 5 μL of a saturated solution of 2,5-dihydroxybenzoic acid in $CHCl_3$; 1 μL of the resulting solution was deposited on a stainless steel sample holder and air-dried. External calibration was provided by the $[M + H]^+$ ions of Angiotensin II (*m*/*z* 1046) and 2,5-dihydroxybenzoic acid (*m*/*z* 155).

Infrared Spectroscopy. Infrared absorption spectra were recorded as KBr pellets by Fourier transform infrared spectroscopy (FTIR) (Perkin-Elmer 2000), in the range 6500−400 cm^{-1}, with a resolution of ±1 cm^{-1}.

UV−Vis Spectroscopy. UV−vis spectra of the coating films, in the range 190−800 nm, were recorded by a UV−vis spectrophotometer (Perkin-Elmer 3λ).

(20) Bax, A.; Subramanian, S. *J. Magn. Reson.* **1986**, *67*, 565.
(21) (a) Otting, G.; Wüthrich, K. *J. Magn. Reson.* **1988**, *67*, 569. (b) Drobny, G.; Pines, A.; Sinton, S.; Weitekamp, D.; Wemmer, D. *Faraday Symp. Chem. Soc.* **1979**, *13*, 49.

Scheme 1. Schematic Drawing of the Nonhydrolytic−Hydrolytic Procedure of Preparation

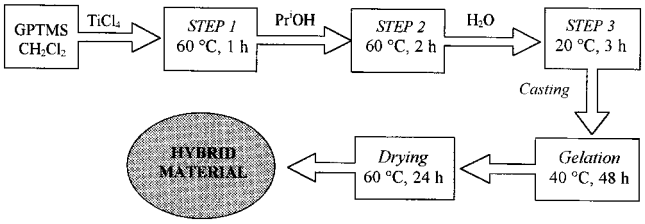

Chart 1. (3-Glycidoxypropyl)trimethoxysilane (GPTMS)[a]

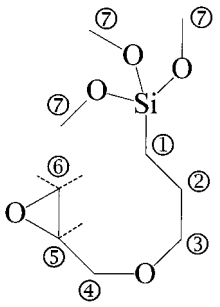

[a] Only protons in position ⑤ and ⑥ are depicted. NOESY experiments suggest the particular conformation given to the molecule.

Results

The addition of $TiCl_4$ to GPTMS in CH_2Cl_2 at room temperature resulted in an immediate color change of the sol from colorless to yellow, with significant evolution of heat, indicating that immediate exothermic reactions occurred. The viscosity also increased in a few minutes under heating, and the solution turned into a spinnable sol (step 1). After 30 min from the addition of $TiCl_4$, precipitation occurred in the case of GTi2 sol. Therefore, the synthesis was completed by steps 2 and 3 only for GTi1. Pr^iOH dissolved the viscous sol without phase separation (step 2). Upon addition of water, the sol remained yellow without the presence of any precipitate (step 3). The procedure of preparation is summarized in Scheme 1.

Characterization of GPTMS. First, the ^{1}H and ^{13}C spectra of GPTMS were recorded (Figures 1a, 2a, 3a, and 4a). 2D NMR spectroscopy allowed the assignment of all the resonance peaks (Chart 1). The ^{1}H and ^{13}C chemical shift (δ) and first order ^{13}C−^{1}H scalar coupling constants ($^1J_{CH}$) are listed in Table 1. The values are in agreement with previous reports.[17] From NOESY measurements (not reported), one can observe (a) an interaction between H_5 and only one of the protons H_6 and $H_{6'}$, so that the signal at ca. 2.6 ppm is assigned to the hydrogen in the syn orientation with respect to H_5, (b) an interaction between H_{6anti} and just one of the H_4 nuclei, (c) an interaction between H_1 and H_{6syn}, and (d) interactions of different intensities between the H_3 and $H_{4,4'}$ nuclei. These results allowed us to propose the average molecular conformation shown in Chart 1.

Characterization of GTi1 and GTi2 Sols after Step 1. The GTi1 and GTi2 sols resulting from the reaction of GPTMS with $TiCl_4$ (step 1) have been characterized by ^{1}H, ^{13}C, and ^{29}Si NMR, GC-MS, and ESI experiments.

Table 1. List of ^{1}H and ^{13}C Chemical Shifts (δ) and of First-Order ^{13}C−^{1}H Scalar Coupling Constants ($^1J_{CH}$) for the Unreacted GPTMS Molecule, with Objective Assignments[a]

	group posn						
	≡SiCH$_2$– ①	–CH$_2$– ②	–CH$_2$O– ③	–OCH$_2$– ④	–CHO– ⑤	–OCH$_2$– ⑥	–OCH$_3$ ⑦
δ(^{1}H) (ppm)	0.58	1.59	3.40	H$_4$: 3.23 H$_4$: 3.64	3.07	H$_{6syn}$: 2.67 H$_{6anti}$: 2.48	3.45
δ(^{13}C) (ppm)	t, 5.45	t, 23.16	t, 73.61	t, 71.88	d, 50.91	t, 44.02	q, 50.41
^1J(CH) (Hz)	117	127	141	142	172	175	143

[a] Numeration is referred to Chart 1.

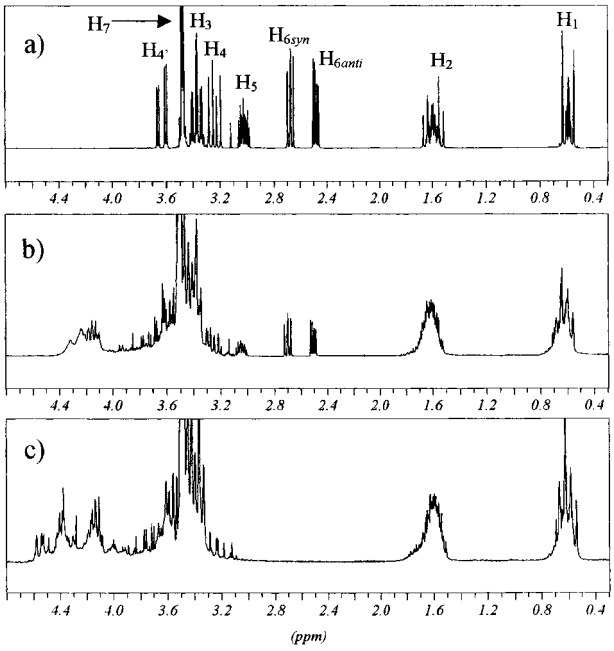

Figure 1. ^{1}H NMR spectra of GPTMS (a), GTi1 sol (b), and GTi2 sol (c) after reaction step 1. The attributions are referred to Table 1.

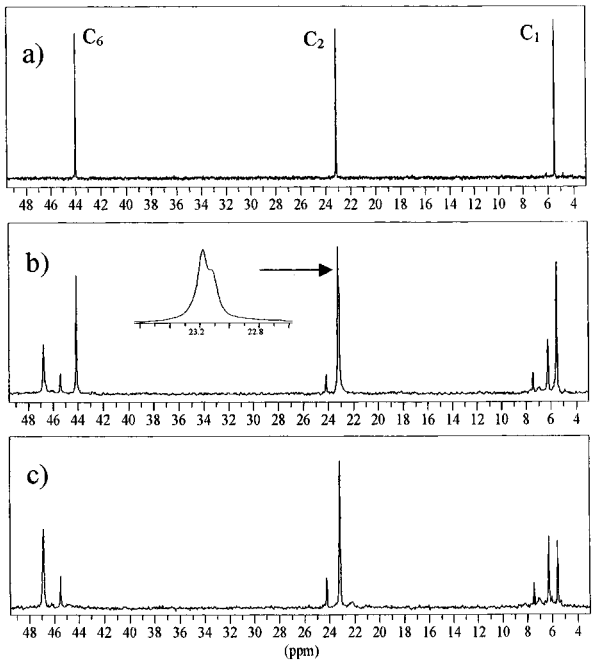

Figure 2. ^{13}C NMR spectra expanded in the 3−49 ppm region of GPTMS (a), GTi1 sol (b), and GTi2 sol (c) after reaction step 1. The attributions are referred to Table 1.

The ^{1}H NMR spectra of sol GTi1 (Figure 1b) and GTi2 (Figure 1c) after step 1 show a continuous decrease of the peaks due to H_5 and H_6 (Scheme 2 and Table 1), while several new multiplets are now present at 0.59, 1.60, 3.30, 3.80, and 4.10−4.30 ppm. This suggests the opening of the epoxy ring with $TiCl_4$ addition. For Si/Ti = 8 (GTi1), the extent of ring opening was estimated to about 60%; for Si:Ti = 4 (GTi2), the reaction is complete. This ring opening reaction seems to occur with the formation of several new species, which we have attempted to identify through a ^{13}C NMR study.

The ^{13}C spectra of GTi1 and GTi2 sols after step 1 are presented in several figures (Figures 2−4) for clarity. In the 3−49 ppm region, the GPTMS spectrum (Figure 2a) shows three signals at 5.45, 23.16, and 44.02 ppm, which are assigned respectively to the C_1, C_2, and C_6 carbon atoms (Chart 1). As expected from the ^{1}H NMR results, the C_6 peak due to the epoxy ring strongly decreases in GTi1 sol (Figure 2b) and totally disappears in GTi2 (Figure 2c). But the peaks due to C_1 and C_2 atoms remain, suggesting the presence of GPTMS-derived species in which only the opening of the epoxy ring occurs, without affecting the chemical shift of the C_1 and C_2 atoms. Other species are also formed, as indicated by the presence of two sets of new signals. ^{13}C−^{1}H heterocorrelation experiments, combined with signal integration, show that these new signals can be attributed to two species containing the Si−CH$_2$–CH$_2$ moiety. The most abundant species is characterized by signals at 6.19 (t, J_{CH} = 118 Hz), 23.10 (t, J_{CH} = 127 Hz), and 46.79 ppm (t, J_{CH} = 151 Hz), while the minor one exhibits signals at 7.39 (t, J_{CH} = 116 Hz), 24.16 (t, J_{CH} = 127 Hz), and 45.41 ppm (t, J_{CH} = 151 Hz). The chemical shift of the C_γ atom, 45−47 ppm instead of 73.6 ppm in GPTMS, strongly suggests a cleavage of the (Si−CH$_2$–CH$_2$−)CH$_2$–O bond and the formation of CH$_2$–CH$_2$–Cl groups. Indeed, a ^{13}C−^{1}H heterocorrelation experiment shows that the signal observed at 46.79 ppm is connected to geminal protons of chemical shift in the range 3.60−3.45 ppm and can be attributed to the terminal −*C*H$_2$Cl moiety bonded to an asymmetric carbon. The presence of these groups suggests chlorination of the organic chains and/or fragmentation of the 3-glycidoxypropyl groups.

In the 48−52 ppm region, the GPTMS spectrum (Figure 3a) shows two signals at 50.91 and 50.41 ppm, due respectively to the C_5 carbon atom in the epoxy ring, which disappears upon addition of $TiCl_4$, and to the methoxy C_7 atom. In GTi1 (Figure 3b), the signal of methoxy carbon atoms is accompanied by another broad peak at 50.65 ppm (q, $^1J_{CH}$ = 143 Hz), which increases in intensity when a double amount of $TiCl_4$ is used (GTi2, Figure 3c). This suggests the formation of various new methoxysilane species, certainly in relation with the formation of the new species discussed above.

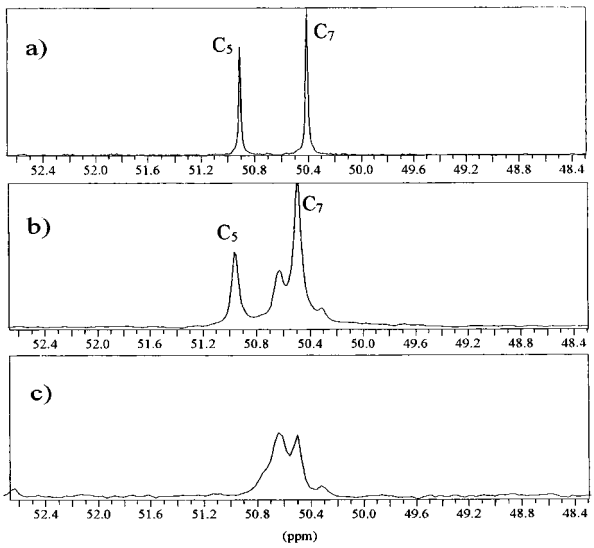

Figure 3. Same as in Figure 2 but for the 48−52 ppm region. The attributions are referred to Table 1.

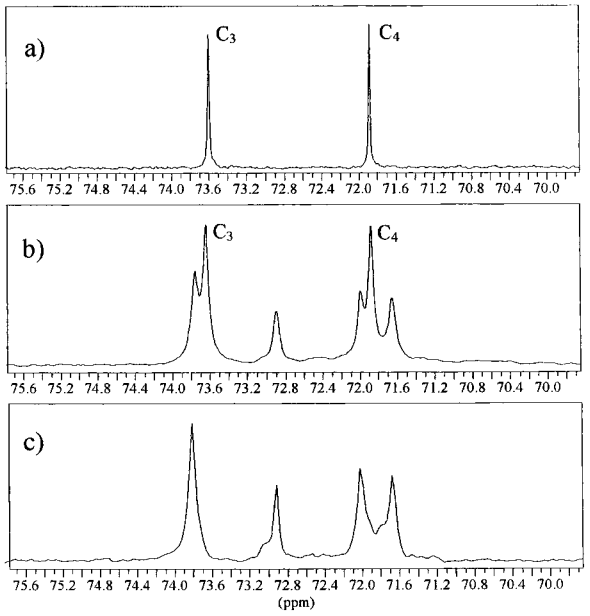

Figure 4. Same as in Figure 2 but for the 61−76 ppm region. The attributions are referred to Table 1.

In the 61−76 ppm region, the GPTMS spectrum (Figure 4a) shows two signals at 73.60 and 71.88 ppm due to the ethereal C_3 and C_4 atoms (Chart 1), which decrease in intensity in the GTi1 and GTi2 sols (Figure 4b,c). New peaks appear at 73.80 ppm (t, $^1J_{CH}$ = 141 Hz), 72.91 ppm (t, $^1J_{CH}$ = 142 Hz), 72.00 ppm (t, $^1J_{CH}$ = 142 Hz), and 71.65 ppm (d, J_{CH} =145 Hz). These chemical shift values are still characteristic of ethereal O−CH and O−CH_2 groups and may suggest polymerization reaction. In GTi1, low-intensity broad signals are also detected at 63.08, 63.86, and 65.05 ppm. They are correlated to a broad proton signal in the range 4.0−4.3 ppm; they are attributed by comparison with data reported in the literature[22] to methoxy groups bonded to Ti. The same species were also detected in GTi2 (not shown in the figure).

(22) Clegg, W.; Elsegood, M. R. J.; Errington, R.; Havelock, J. *J. Chem. Soc., Dalton Trans.* **1996**, 681.

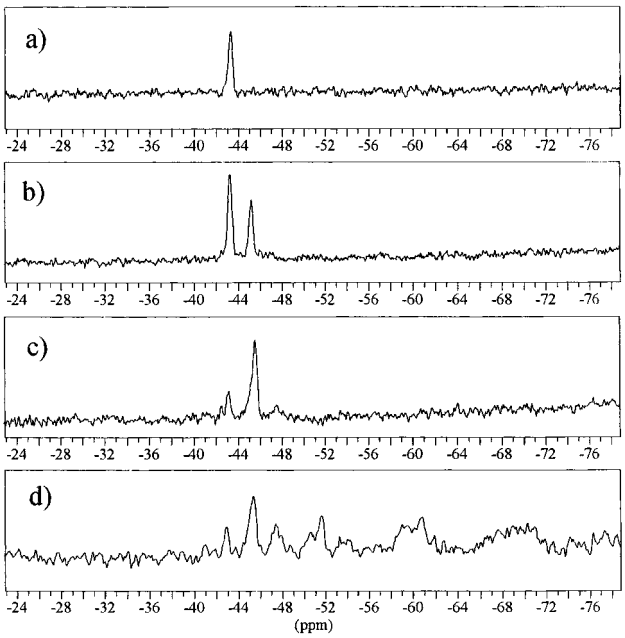

Figure 5. ^{29}Si NMR spectra of GPTMS (a) and GTi1 sol after step 1 (b), step 2 (c), and step 3 (d).

After step 1, the ^{29}Si NMR spectrum shows an additional peak at −45.2 ppm when compared to the spectrum of GPTMS, characterized by one resonance peak at −43.3 ppm (Figure 5a,b). This chemical shift value still corresponds to a trialkoxysilane, which indicates the retention of the Si−CH_2 bonds after addition of $TiCl_4$; however, the shift in peak position should be due to the formation of new species with a modified Si environment.

GC-MS analysis of reaction mixture GTi1 after step 1 is shown in Figure 6. The peak at 15.10 min shown in the chromatogram (Figure 6a) contains two unresolved species, which are detected in the corresponding mass spectrum (Figure 6b). The base peak at *m/z* 209 is accompanied by a peak at *m/z* = M + 2 (*m/z* = 211) indicating the presence of a chlorine atom: this species loses a propene molecule giving rise to an ion with *m/z* = 167. The same spectrum shows also a peak at 197 *m/z*, accompanied by a peak at *m/z* = M + 2 (*m/z* = 199), which loses a chlorine producing an ion with *m/z* = 163 and subsequent peaks result from successive loss of CH_2 groups. By comparison with the ^{29}Si NMR results, these results suggest the presence of at least two organosilane species after step 1 in GTi1 sol, both of them containing one chlorine atom, and corresponding to *m/z* = 209, 211 and *m/z* = 197, 199. ESI mass analysis of the same GTi1 sol (Figure 7) shows the presence of species at *m/z* 519 and 645, which have been attributed[2323] also on the basis of the isotopic cluster analysis to the formation of methoxy titanium clusters of type

$$CH_3O-[Ti(OCH_3)_{2-}O]_n-Ti^+(OCH_3)_2$$

with *n* = 3 and 4, respectively. The species at *m/z* 645 can lose a neutral tetramethoxytitanium, leading to *m/z* = 473 ions, while the peak at *m/z* = 691 is attributed[23] to

$$[Ti_6O_5(OCH_3)_6(OH)_8H]^+$$

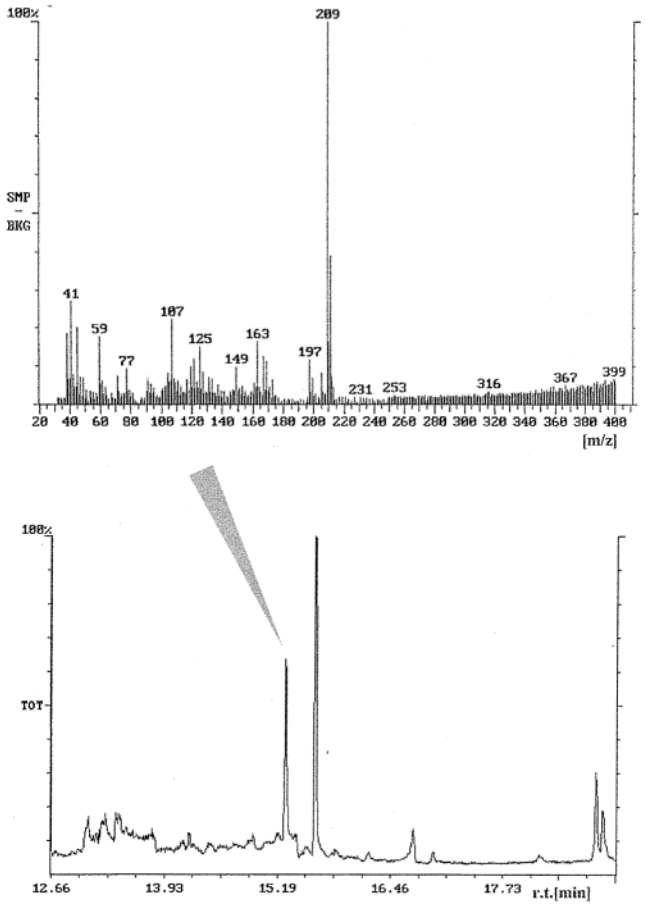

Figure 6. GC-MS analysis of GTi1 after step 1. The mass spectrum (b) is relative to species at 15.10 min with base peak at *m*/*z* 209.

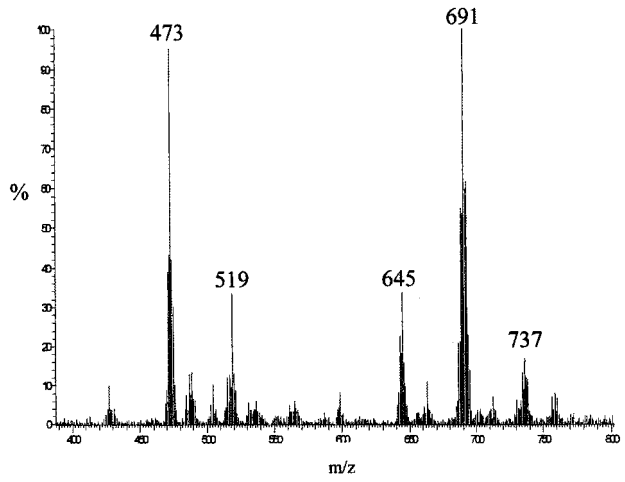

Figure 7. ESI mass analysis of GTi1 after step 1.

This is in agreement with the ^{13}C NMR results that have suggested the formation of Ti−OMe bonds.

Characterization of GTi1 Sols after Steps 2 and 3. After steps 2 and 3, which correspond to a dilution with an excess of 2-propanol followed by hydrolysis, the ^{13}C NMR spectra of the GTi1 sol have been recorded (Figure 8). In the region due to the C_α atoms, the three signals present after step 1 (Figure 2b) are now split in various components after dilution (Figure 8a). This

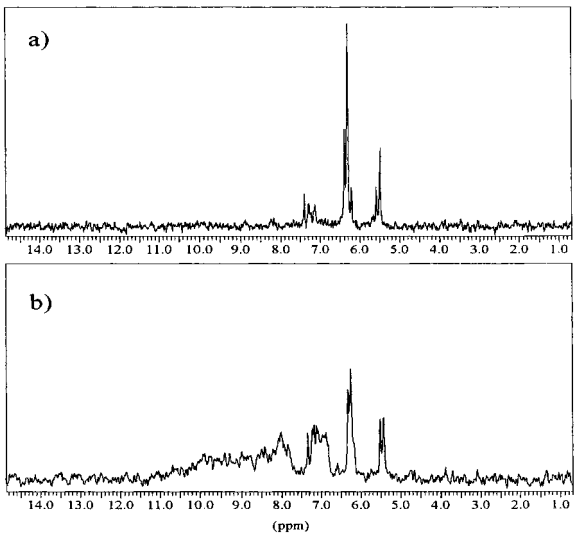

Figure 8. ^{13}C NMR spectra of GTi1 after step 2 (a) and step 3 (b).

strongly suggests exchange reactions between the methoxy groups and the isopropoxy groups, leading to the formation of $-CH_2-Si(OMe)_{3-x}(OPr^i)_x$ ($x = 1-3$). After hydrolysis, broad peaks appear in the 6−10 ppm range (Figure 8b), which reflects the change in the Si environment, during the hydrolysis−condensation process, which transforms the alkoxy groups into OH groups and then oxo bridges.

The ^{29}Si NMR spectrum recorded after step 2 (Figure 5c) on the GTi1 sol shows a decrease in intensity of the peaks at −43.3 and −45.2 ppm respectively assigned to GPTMS and a new trialkoxysilane species. This last peak is now overlapped by a new one, resulting in a signal centered at −45.6 ppm. A minor peak is also detected at −47.55 ppm. Those peaks may be assigned to the presence of mixed $-CH_2-Si(OMe)_{3-x}(OPr^i)_x$ ($x = 1-3$) units, as suggested above. After step 3 (Figure 5d), these species are still present, together with condensed ones, characterized by broad signals around −51, −60, and −69 ppm. These values are characteristic of T_1-T_3 species that correspond respectively to Si units with 1−3 oxo bridges. The presence of residual alkoxy groups can be explained by the low hydrolysis ratio that was used (H_2O:GPTMS = 1:1) to avoid precipitation during the synthesis.

Characterization of GTi1 Powders. The ^{29}Si MAS NMR spectrum recorded on the final GTi1 (not in figures) shows the total disappearance of the monomeric species. The main signal at −67 ppm (52%) is due to fully condensed Si units from GPTMS (T_3 units), while the two peaks at −59 ppm (40%) and −51 ppm (8%) revealed the presence of residual T_2 and T_1 units. This corresponds to a well-condensed network, with a degree of condensation of 81%.

The FTIR spectra of GT and GTi1 powders are shown in Figure 9 in the range 3115−3020 cm^{-1}, where a characteristic IR absorption band of C−H stretching vibration of the epoxy ring is detected.[24] This band is

(23) Cristoni, S.; Armelao, L.; Gross, S.; Tondello, E.; Traldi, P. *Rapid Commun. Mass Spectrosc.* **2000**, *14*, 662.

(24) (a) *Comprehensive Heterocyclic Chemistry*; Lwoswsi, W., Ed.; Pergamon Press: Oxford, U.K., 1984; Vol. 7, p 99. (b) *Atlas of Spectral Data and Physical Constants for Organic Compounds*; Grasselli, J. G., Ritchey, W. M., Eds.; CRC Press Inc.: Cleveland, OH, 1975; Vol. 1.

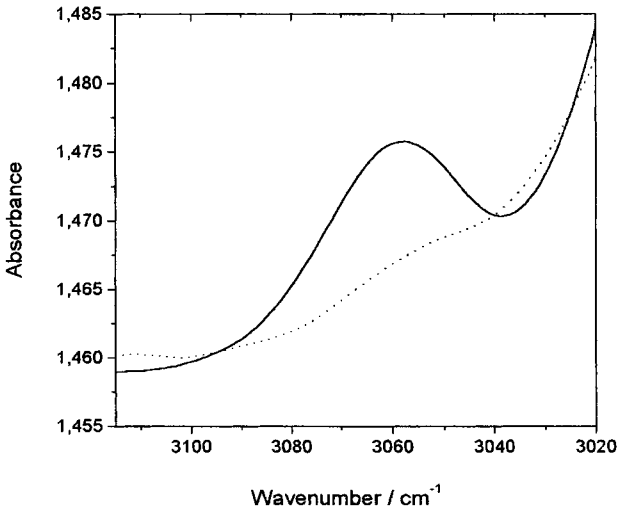

Figure 9. FTIR spectra of GT (continuous line) and GTi1 (dotted lines) powders in the 3020−3115 cm^{-1} range.

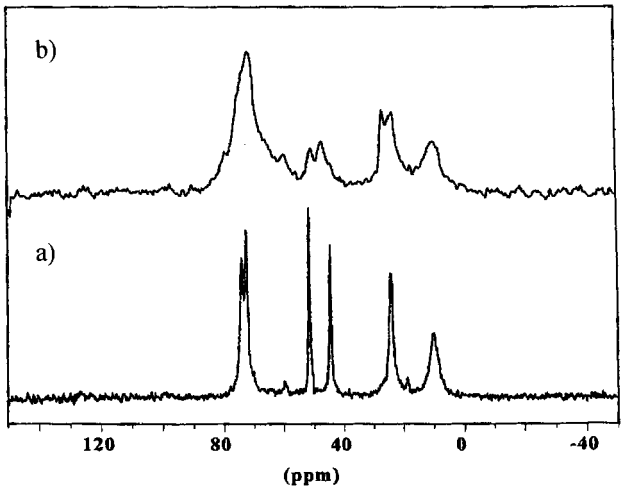

Figure 10. ^{13}C CP MAS NMR spectra obtained on GT (a) and GTi1 (b) powders.

intense in GT but is only weakly detected in GTi1. This allows us to estimate that around 85% of the epoxy rings have been opened with respect to GT. Figure 10 compares the ^{13}C CP MAS NMR spectra obtained on the same samples. The peaks observed for GT are characteristic of unpolymerized glycidoxypropyl groups,[15] at 9.6 ppm (C_1), 23.8 ppm (C_2), 44.2 ppm (C_6), 51.3 ppm (C_5), and 72.3 and 73.8 ppm (C_4 and C_3) (see Table 1). The peak due to C_1 is in the same chemical shift range as the broad peaks that appear after the hydrolysis step 3 (Figure 8b). The shift from 5.45 ppm in GPTMS to 9.6 ppm in GTi1 powder is thus clearly due to the replacement of alkoxy groups by oxo bridges. The two sharp peaks due to mobile epoxy rings (C_5 and C_6) have disappeared, while an intense broad peak is now present around 71 ppm due to polymerized ethylene oxide species $(-O-CH_2-CH_2)_n-$. One signal is present at 50 ppm with a shoulder at 44 ppm that could be due to residual epoxy rings in agreement with the FTIR results. The higher intensity of the peak at 50 ppm, with respect to that at 44 ppm, may suggest the presence of an extra signal at 50 ppm that may be due to methoxy groups. The peak detected at 26 ppm is certainly due to isopropoxy groups. The CH signal of such moieties is

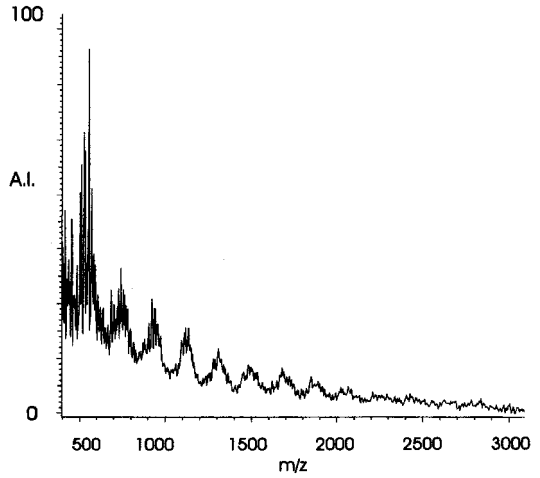

Figure 11. MALDI mass analysis of the GTi1 final powder.

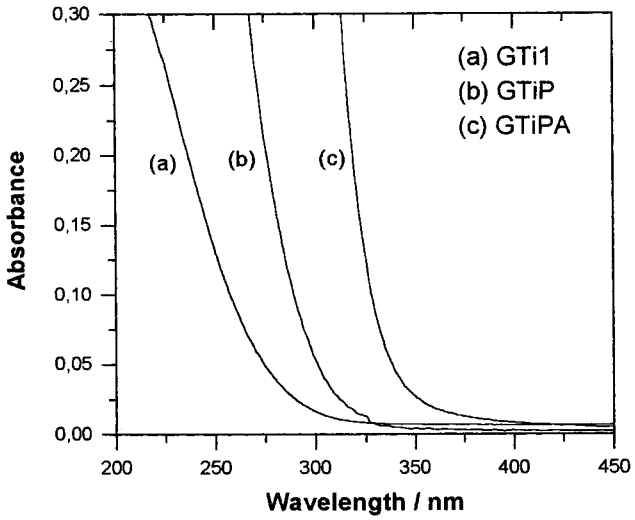

Figure 12. UV−vis spectra of GTi1 films (a). The absorption spectra of films prepared from GPTMS using $Ti(OPr^i)_4$ without (GTiP) and with acetylacetone (GTiPA) are reported for comparison, spectra (b) and (c), respectively.

expected[27] around 66 ppm for $Si-OPr^i$ or 76 ppm for $Ti-OPr^i$. In each case, it will be overlapped by the broad signal due to the poly(ethylene oxide) chains. More interesting is the peak detected at 47 ppm: according to the solution state study, it may be due to some CH_2Cl moieties.

The MALDI spectrum obtained in the final gel (Figure 11) illustrates the degree of organic polymerization reached in the solid state, with the presence of poly(ethylene oxide) oligomers until MW about 2500 uma. The repeating units with a MW of 190 uma correspond to 3-glycidoxypropyl$-SiO_3$.

The UV−Vis spectrum of GTi1 films is shown in Figure 12. The spectra of GPTMS$-TiO_2$ samples prepared from $Ti(OPr^i)_4$ with (samples GTiPA) or without acetylacetone (samples GTiP) are reported for comparison. The GTi1 spectrum shows a low absorbance in the visible range and a shift of the UV absorption edge to lower wavelengths with respect to GTiPA and GTiP.

(25) Bourget, L.; Corriu, R. J. P.; Leclercq, D.; Mutin. P. H.; Vioux, A. *J. Non-Cryst. Solids* **1998**, *242*, 81.
(26) Bégué, J. P.; Benayoud, F.; Bonnet-Delpon, D. *J. Org. Chem.* **1995**, *60*, 5029.
(27) Diré, S.; Babonneau, F. *J. Non-Cryst. Solids* **1994**, *167*, 29.

Scheme 2. Processes Occurring during Step 1

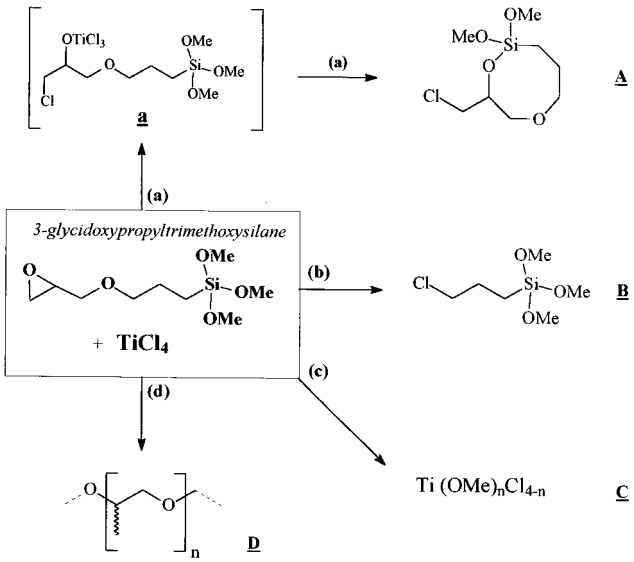

Discussion

1. Nonhydrolytic Reaction of $TiCl_4$ with GPTMS. According to the NMR and MS results, the reaction of $TiCl_4$ with GPTMS under nonhydrolytic conditions results in a series of different chemical interactions between the two compounds, which can be summarized as follows: (1) opening of the epoxy rings; (2) formation of poly(ethylene oxide) chains; (3) cleavage of the glycidoxypropyl groups; (4) formation of $Si(CH_2)_3Cl$ moieties; (5) the presence of $TiCl_n(OMe)_{4-n}$ clusters. Indeed, as reported in the literature, the highly reactive $TiCl_4$ was expected to interact with the oxygen sites in GPTMS without breaking the $Si-CH_2$ bonds[25] and this behavior was indeed confirmed by the ^{29}Si NMR spectra.

$TiCl_4$ can react with different sites in GPTMS: (a) oxygen atom of the epoxide ring; (b) ethereal chain oxygen; (c) oxygen atoms of Si−OMe groups.

$TiCl_4$, as reported in the literature,[26] is expected to react with epoxy ethers at the epoxide oxygen with subsequent preferential attack of Cl^- to the less hindered carbon, forming cyclic or acyclic products,[26] depending on the reaction conditions. The ring opening of GPTMS by $TiCl_4$ can occur by addition of a Cl atom to the carbons of epoxide ring preferentially on the less hindered CH_2 group, giving rise to species of type ***a*** shown in Scheme 2. The $-OTiCl_3$ group represents a reactive site which can further attack the OMe group on silicon, so that cyclic molecules migth be formed (i.e. ***A***) as well as $TiCl_n(OMe)_{4-n}$ species (***C***). The formation of cyclic alkoxides (***A***) is, however, not unambiguously demonstrated by experimental evidence, even if the conformation proposed in Scheme 2 for GPTMS, on the basis of NOESY measurements, supports the hypothesis of the formation of cyclic derivatives. But indeed, the presence of the species ***A*** is in perfect agreement with the NMR and GC-MS experiments. The ^{13}C NMR signals at 72.00, 73.80, and 71.65 ppm can be attributed, on the basis of signal integration and on heterocorrelation experiments, to the ethereal CH_2-O-CH_2 groups and to the *C*H carbon, respectively (Figure 4). The other carbon atoms display resonance peaks at 46.79 ppm for the terminal $-CH_2Cl$ group and at 6.19 and 23.10 ppm for the $-CH_2-$ groups (Figure 2). The OMe groups appear as a broad signal at 50.66 ppm that increases when the amount of $TiCl_4$ is doubled to obtain a complete ring opening (Figure 3). An indication of species of type ***A*** is also obtained by the GC-MS analysis (Figure 6). The peak at *m*/*z* 209 corresponds to a fragment formed from ***A*** after the loss of a OMe group. The presence of a chlorine atom and the loss of a propene support the cyclic structure ***A*** (Scheme 2). The second well-detectable set of ^{13}C NMR signals at 7.39, 24.16, and 45.41 ppm (Figure 2) can be attributed to the product ***B*** obtained from the reaction of $TiCl_4$ with the ethereal chain oxygen (route b of Scheme 2). The MS analysis of the reaction mixture (Figure 6) confirms the presence of this second species, with a peak at *m*/*z* 197 (M + 2, *m*/*z* 199), which can lose a chlorine atom and then subsequently CH_2 groups.

Finally, a broad triplet on the coupled ^{13}C NMR spectrum at 72.90 ppm ($^1J_{CH}$ = 142 Hz) can be attributed to the oligomerization of the epoxide ring (Figure 8), as reported in route d of Scheme 2. This value is in agreement with the data obtained in the presence of BF_3.[19]

The ^{29}Si NMR spectrum (Figure 5b) also agrees with these assumptions: the peak at −43.3 ppm can be due to GPTMS but also to species ***B*** and ***D***. The peak at −45.18 ppm can be attributed to species ***A***, in agreement with the data reported in the literature when a methoxy group is replaced with a larger group such as isopropoxide.[27] No clear evidence for Si−Cl and Si−O−Ti species can be obtained.

2. Hydrolytic Reactions. The dilution of the reaction mixture in 2-propanol (step 2) first causes an exchange reaction between the Si−OMe and the Si−OPr^i groups. Then, the addition of water in substoichiometric amount at room temperature (step 3) induces the hydrolysis and condensation of the inorganic silicon moiety and also of Ti centers. All these results are in agreement with the ^{13}C and ^{29}Si solution-state NMR results. After gelation and drying, both organic and inorganic polymerization occur to a large extent: the ^{29}Si MAS NMR spectrum reveals a high degree of condensation for the siloxane network while the ^{13}C MAS NMR spectrum shows a broad peak due to poly(ethylene oxide) chains. Indeed, all the ^{13}C resonance peaks are broad, indicating the rigid amorphous character of the sample compared to the GT sample in which no organic polymerization occurred. An estimation of the corresponding molecular weight of the polymer chains is indeed given in the MALDI experiment. The polymerization reactions which started during step 1, i.e., before hydrolysis, indeed did not prevent the inorganic condensation reactions to occur to a large extent, leading to a highly cross-linked network. The ^{13}C MAS NMR spectrum suggests the presence of CH_2-Cl groups, which could indicate chlorination of the organic chains and/or fragmentation of the 3-glycidoxypropyl groups.

An indication of the level of dispersion of titanium within the matrix is given by the UV−vis spectra (Figure 12). The UV−vis absorption edge wavelength is correlated with the dimensions of titania nanoaggregates, according to the literature,[28−31] which are formed

(28) Kormann, C.; Bahnemann, D. W.; Hoffmann, M. R. *J. Phys. Chem.* **1988**, *92*, 5196.

in the matrix as a consequence of a phase separation during the synthesis. A shift of the absorption edge to lower wavelengths is in fact attributed to a reduced dimension of these nanoaggregates.[28−31] The large differences observed among GTi1, GtiP, and GTiPA UV−vis spectra can be attributed to different dimensions of TiO_2 clusters much reduced in GTi1. This in comparison to hybrid materials obtained from titanium alkoxides could be achieved by this new synthesis method.

Conclusions

(3-Glycidoxypropyl)trimethoxysilane-derived hybrid materials were synthesized by $TiCl_4$ that was used in nonhydrolytic conditions to achieve epoxy ring opening polymerization by a multistep reaction. In the first step $TiCl_4$ was added to GPTMS in CH_2Cl_2; at this stage efficient promotion of epoxide ring opening of GPTMS was reached at room temperature and in short reaction times. After the addition of $TiCl_4$ to GPTMS in nonhydrolytic conditions, several new species and poly(ethylene oxide) oligomers were formed, as revealed by NMR analysis. These molecules bear a monochlorinated hydrocarbonic tail and on addition of water, in the last step of reaction, undergo hydrolysis−condensation reactions, to give an inorganic network. Linear compounds of different lengths were formed. The final material deposited as a coating film showed a high transparency in the UV−vis range.

CM011034O

(29) Brus, L. *J. Phys. Chem.* **1986**, *90*, 2555.
(30) Sorek, Y.; Reisfeld, R.; Weiss, A. M. *Chem. Phys. Lett.* **1995**, *244*, 371.
(31) Brusatin, G.; Guglielmi, M.; Innocenzi, P.; Martucci, A.; Battaglin, G.; Pelli, S.; Righini, G. C. *J. Non-Cryst. Solids* **1997**, *220*, 202.